Desalination and Water Treatment
www.deswater.com

doi: 10.5004/dwt.2022.28090

248 (2022) 28–38
February

Initiation and inhibition of pitting corrosion on C-steel in oilfield-produced water under natural corrosion conditions

S. Abd El Wanees[a,b,*], M.M. Kamel[c], S.M. Rashwan[c], Y. Atef[d], M.G. Abd El Sadek[e]

[a]*Chemistry Department, Faculty of Science, Zagazig University, Zagazig 44519, Egypt, email: s_wanees@yahoo.com (S. Abd El Wanees)*
[b]*University College of Umluj, University of Tabuk, Tabuk, Saudi Arabia, email: s_nasr@ut.edu.sa*
[c]*Chemistry Department, Faculty of Science, Suez Canal University, Ismailia, Egypt, email: madhet_kamel@yahoo.com (M.M. Kamel)*
[d]*Research Laboratory, Egyptian Chemistry Administration, Cairo, email: jasy9@yahoo.com (Y. Atef)*
[e]*Research and Chemicals Department, General Petroleum Company, GPC, Nasr City, Cairo, email: msadek.2004@gmail.com (M.G. Abd El Sadek)*

Received 22 July 2021; Accepted 4 December 2021

ABSTRACT

The initiation and inhibition of the localized pitting corrosion on the C-steel surface in oilfield-produced water are investigated by pitting corrosion current measurements. The current-time curves are characterized by the appearance of an induction period, τ followed by a rapid rise in the pitting corrosion current till reaches the limiting value, I_L, due to propagation of pitting corrosion. The I_L value reaches 5.0 μA cm^{-2} in 99% diluted oilfield-produced water and 260 μA cm^{-2} in pure oilfield-produced water. The presence of HPO_4^{-2}, WO_4^{-2}, and MoO_4^{-2} anions suppresses the initiated current by elongation of the induction time, τ. Such anions acted as inhibitors towards the pitting corrosion of the C-steel. The inhibition efficiency, η, of the studied inhibitors increases in the following order: Na_2WO_4 < Na_2MoO_4 < Na_2HPO_4. The inhibition mechanism is assumed to take place through an adsorption process obeying Langmuir's model. The thermodynamic parameters for the adsorption process K_{ads} and ΔG°_{ads} are calculated and discussed.

Keywords: Oilfield-produced water; C-steel; Pitting corrosion; Inorganic passivator; Adsorption

1. Introduction

Nearly all oil production wells have chloride and sulfate salts mixed with the production water or emulsified with crude oil causing a dangerous type of pitting corrosion for steel equipment utilized in oil and gas production. Equipment prepared from C-steel can be attacked easily by aggressive anions which are naturally contaminated the formation water. The presence of chloride and sulfur ions which are abundant in the underground water can easily severe corrosive problems in frameworks such as equipment and pipelines in processes of recycling and reuse of produced water that leads to considerable economic losses.

Several corrosion inhibitors are added to oilfield-production water during petroleum output for controlling the destructive effect of the corrosive anions which are mixed with the produced water environment. A broad of corrosion inhibitors are utilized to reduce the corrosion of the steel in the various corrosive media [1–8]. Generally, most of the used inhibitors are organic and inorganic materials, which generally form a protective layer on the metal surface. The unused inhibitors are released into the environment as an aqueous waste and thus affect the living organisms due to the toxic properties of some of the used chemicals. The use of inorganic inhibitors as an alternative

* Corresponding author.

to organic compounds is based on the possibility of degradation of organic compounds with time and temperature [9,10].

Various inorganic salts are utilized as effective inhibitors or passivators for various metals and metal alloys in different electrolytes [11–17]. As a result of the poisonous effect of most of these ions, it limited the toxic use of these anions. Therefore, safe anions without any polluted effect were chosen as inhibitors such as Na_2HPO_4, Na_2MoO_4, and Na_2WO_4 towards the corrosion of C-steel in oilfield-production water.

In our study, the influence of the oilfield produced-water obtained from North East Sannan, NES-4, in the Western Desert, Egypt, in a depth of 2,415–2,435 m on the induced pitting corrosion of C-steel was studied. The investigation was carried out by using a simple cell constructed early for measuring the localized pitting corrosion current under natural corrosion conditions [13,18–20].

2. Experimental

2.1. Materials and the electrolytic cell

The used electrodes were prepared from carbon steel C1018. The elemental analysis of the steel samples was estimated, as weight percent, by Tabbin Institute for Metallurgical Studies (TIMS), Helwan–Cairo, Table 1.

The C-steel electrodes were reinforced to Pyrex-glass pipes using Araldit resin leaving a free cross-sectional surface area is 0.04 cm^2. Before each run, the surface of the steel electrodes was mechanically abraded using various grades of polished papers, rinsed with acetone, and finally washed with doubly distilled water.

Due to localized pitting corrosion on most metals and steel surfaces, the pitting corrosion current can be measured using a simple electrolytic cell that is described early, Fig. 1 [13,18–20]. The cell was made of a double wall borosilicate glass with a volume of 100 cm^3 solution and comprising a C-steel electrode, A, as an anode. The cathode was a similar C-steel electrode with the same surface area and elemental composition, B. The cathode was enclosed in a borosilicate glass tube ending with a fine porosity fritted centered glass disc G_4, C, and included in the cell container. A copper wire was used for connection between the steel electrodes using a nano-amperemeter device (Siemens type N-5536).

2.2. Corrosive electrolyte, oilfield-produced water

Generally, deep oilfield-produced water is liberated in the reservoir rocks before drilling. Such water utilized in our study was gained from one of the wells of the general petroleum company, GPC, Egypt, in the Western Desert, North East Sannan, NES-4 in a depth of 2415–2435 m underground mixed with crude oil. The chemical composition and physical properties of the produced water are given in Table 2.

Two sets of procedures were used. In the first one, the influence of the amounts of the corrosive anions (Cl^- and S) in the oilfield-produced water (FW), expressed by the % of dilution value, on the extent of the produced pitting corrosion current on the C-steel electrode was investigated. Double-distilled water was used to attain the dilution factor of the oilfield-produced water. The prepared electrodes were immersed in the electrolyte, 0.5% oilfield-produced water. Due to the similarity of the electrodes and the electrolytes, no current could be observed while connecting the steel electrodes. After that, the investigated amount of the oilfield-produced water is comprised to the main compartment of the cell, and the initiated current was followed using a nano amperemeter till reaching the limiting current value, I_L [13,18–20].

Table 1
The elemental analysis of utilized steel electrodes, C 1018, in wt.%

S	0.60
Si	0.17
P	0.046
Mn	0.50
C	0.12
Fe	Bal 98.564 mass %

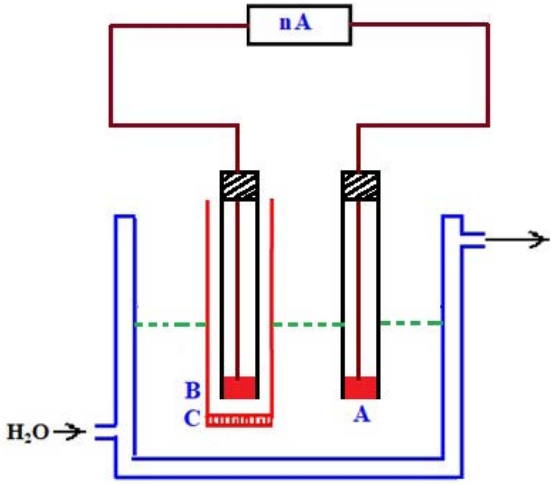

Fig. 1. Electric circuit and electrolytic cell used for pitting corrosion current measurement. A and B are identical C-steel electrodes, C is a fritted centered glass disc G4 and nA is a nano amperometer.

Table 2
Physical and chemical characterization of the oilfield-produced water

Parameter	Value
pH	7.10
Cl^-, ppm	41,477
SO_4^{-2}, ppm	244
Cl^-/SO_4^{-2}	170:1
Ca^{+2}, ppm	2,525
Mg^{+2}, ppm	122
Conductivity, mS cm^{-1}	95.2
Sulfur, %	0.2021
Density, at 25°C, g cm^{-3}	1.03293
Total dissolved salts (TDS), mg L^{-1}	47,600

The other set was conducted with 50% of oilfield-produced water mixed with different additives of the used inorganic salts, Na_2HPO_4, Na_2MoO_4, and Na_2WO_4. Each run was done with freshly prepared electrodes and with a new portion of the examined solution. This was carried out by using the same percent of diluted oilfield-produced water mixed with various additives of the investigated salts. The produced pitting corrosion current was tabulated against the immersion time. To ensure the repeatability of the results, each experiment was duplicated and the data were nearly similar. The average value of the produced current was taken.

The utilized inorganic salts were of analytical grade quality. The examined electrolytes were prepared by using double-distilled water. Experiments were done at room temperature, 25°C ± 0.1°C, excluding those investigated to the various temperatures. The cell temperature was monitored by using an ultra-programmable thermostat (USA).

Scanning electron microscopy of some of the investigated steel electrode samples was done using a JEOL Scanning Microscope, JSM – T100 (Japan).

3. Results and discussion

3.1. Influence of dilution factor on the oilfield-produced water

The corrosion current density produced when the C-steel electrode was immersed in oilfield-produced water was followed against the immersion time till reaching the limiting current, I_L. The curves of Fig. 2 show the behavior recorded in solutions of various diluted oilfield-produced water (polluted by Cl^- and S ions). It is noteworthy to see that, with more diluted oilfield-produced water, 1.0% FW (fewer amounts of the aggressive Cl^- and S ions, very little corrosion current density (5.0 μA cm^{-2}) appears after an induction period extends to 140 min. The current starts to decay due to the passivation of meta-staple pits [21–26]. Such highly diluted oilfield-produced water contains relatively small amounts of aggressive ions (Cl^- and S) that are not sufficient to initiate the pitting corrosion [13,25].

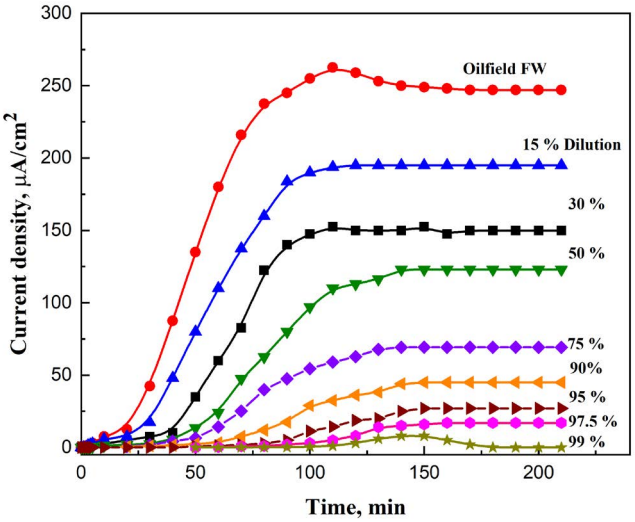

Fig. 2. Current-time curves for C-steel immersed in various diluted solutions of formation water, at 25°C.

At this stage, the passivating anions naturally present in the examined electrolytes such as OH^- and CO_3^{2-} displaced the attacking ions such as Cl^- and S ions at the pit surface causing the decay in the localized pitting current [27]. As the dilution percent of the oilfield-produced water is lowered (an increase in the amount of Cl^- and S ions), the corrosion current starts to increase with decreasing the induction time, τ. In the case of 85.0% FW, the induction time is lowered to 25 min with pitting corrosion current, I_L, reaching 195 μA cm^{-2}, while with pure oilfield-produced water, τ was shorted to ~ 20 min with increasing in the I_L to reach 260 μA cm^{-2}. The appearance of such a high current is an indication of the presence of an electrochemical reaction at the electrode surface [22–26]. Generally, literature has been confirmed that nucleation, growth, and passivation of metastable formed pits on the C-steel surface occur during the formation of metastable pits [28–32]. Some of the formed pits are stable whereas most of them are passivated again. As the rate of pit passivation is lower than that of oxide film destruction, meta-stable pits are supposed to be formed with an increase in the pitting corrosion current [32,33]. Various models about the growth of metastable pits are suggested [33–37]. Early, Williams indicates that the meta-stable pits have a very restricted existence depending on the concentration of the corrosive anions in the oilfield-produced water [34,35]. Subsequently, the pits have been passivated and the initiated current cutout to flow.

However, the increase in the corrosive ions content (Cl^- and S ions) in the oilfield-produced water by decreasing the dilution ratio causes the pitting current to outflow with a decrease in the induction period, τ till reaching the limiting value, I_L. This interval is usually accompanied by the initiation of the localized pitting corrosion [27,28,38,39] and could be related to the time taken by the Cl^- and S ions either to penetrate the passive oxide film [40] or to compete with the passivating anions OH^- and CO_3^{2-} to adsorb on the corroding steel surface [41]. Obvious pits are monitored by screening the surface of the steel electrode, under the scanning electron microscopy (SEM), after running the experiment in 50% diluted oilfield-produced water, Fig. 3. The existence of the Cl^- and S ions give rise to the consistency of intelligible pits. The formed pits take various shapes (fine and moderate in size) and some of them are surrounded by the corrosion products that formed on the electrode surface.

The dependence of the induction time, τ, on the amount of the destructive anions, C_{FW} % (Cl^- and S ions), in oilfield-produced water can be depicted in Fig. 4. The data of such curve performs the logarithmic relation between the two parameters, that is obeying the relation [13,23–26]:

$$\log\tau = \zeta - \lambda \log C_{FW} \quad (1)$$

where ζ and λ are constants that depend on the electrolyte composition and investigated electrode kind. The values of the constants ζ and λ are 173 min and −0.45 log min/decade, respectively.

However, the steady rise in the pitting current could confirm the propagation of the localized pitting corrosion or be attributed to the rise in the number of active pits that are formed on the steel electrode surface with the harmonizing

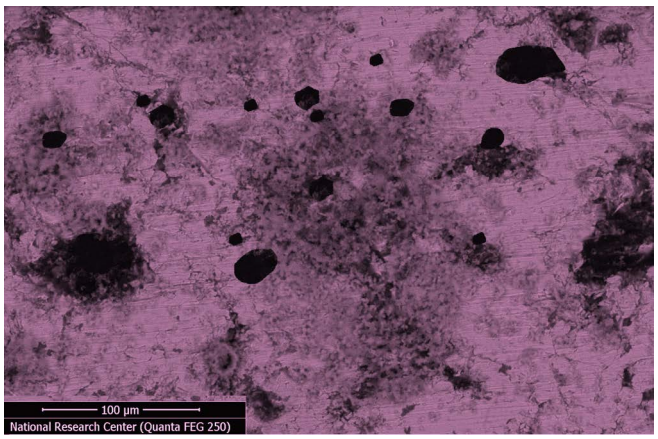

Fig. 3. SEM micrograph of C-steel surface after inundation for 6 h in 50% diluted oilfield-produced water, at 25°C.

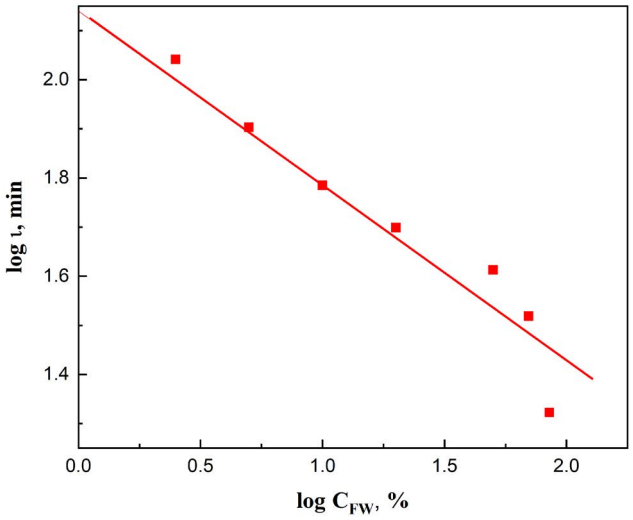

Fig. 4. Variation of the logarithm of the induction period, logτ, on the logC_{FW} % (Cl^- and SO_4^{2-}) for C-steel immersed in various diluted solutions of oilfield formation water, at 25°C.

raise in the total attacked area. The current density eventually attains the limiting value, I_L, which depends on the amount of the aggressive anions in the diluted oilfields-produced water, C_{FW} % (Cl^- and S ions). The attainment of the limiting current signifies that the pitting corrosion of the passive steel electrode takes place at the bottom of the pits formed, whereas their number stays constant [13,23–26]. The rise of the limiting current value upon increasing the C_{FW} % (Cl^- and S ions) implies a rise in the number of the initiated pits, that is, a rise in the anodic area [23]. Fig. 5 confirms the variance of the logarithm of the I_L against the logarithmic concentration of the C_{FW} % (Cl^- and S ions). A straight-line relation is attained following the equation [18,26,34]:

$$\log I_L = \zeta' + \lambda' \log C_{FW}\% \quad (2)$$

where ζ' and λ' are constants that depend on the electrolyte composition and the kind of the investigated metal. The values of ζ' is 0.87 expressed by log µA cm^{-2} while that

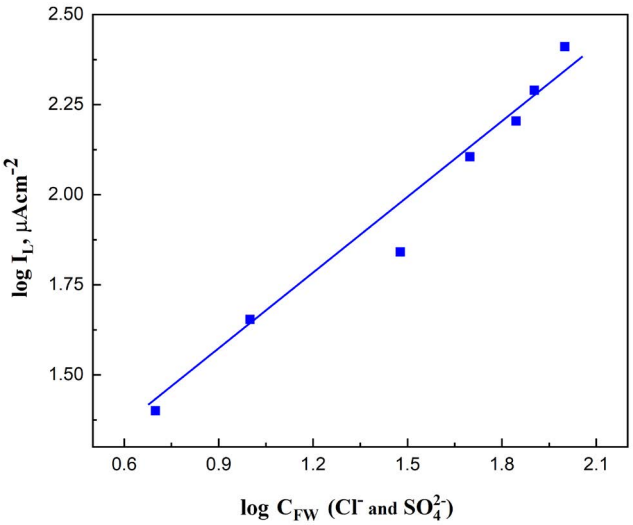

Fig. 5. Variation of the limiting-pitting corrosion current density with the C_{FW} % (Cl^- and SO_4^{2-}) on a double logarithmic scale, at 25°C.

of λ' is 0.71 log µA cm^{-2} $decade^{-1}$. The constant ζ' symbolizes the logarithm of limiting current in case of the existence of 1.0% of aggressive ions. Early studies confirmed that Eq. (2) was deducted theoretically based on the competitive adsorption of the two counteracting anions on the surface of the investigated metal [18,27]. Theoretical derivation indicated that λ' should refer to the value $\alpha_1 n_1/z_1$, where α_1 represents the transfer coefficient of the anodic reaction, n_1 is the number of electrons produced in the oxidation process while z_1 represents the valence of the destructive ions. Generally, α_1 takes values between 0.7 and 0.3 for reactions controlled by transfer across a simple energy barrier. The variation in α_1 values depends on the nature of the reaction that occurs on the electrode surface beside the kind and concentration of the attacking ions [18,27]. Such type of anodic reaction is controlled by a one-electron transfer [18,27]:

$$Fe^{2+} \rightarrow Fe^{3+} + e \quad (3)$$

where n_1 = 1 and z_1 for Cl^- = 1 (and for SO_4^{2-} or S^{2-} = 2) the term $\alpha_1 n_1/z_1$ supposes the values 0.3 as a minimum border and 0.7 as a maximum limit. In our study, the obtained value of 0.71 for the slope of the relationship is mostly in conformity with an anodic reaction of the steel electrode controlled by one-electron transfer [18,27]. The obtained value reaches the upper limit due to the sharing of SO_4^{2-} or S^{2-} as a divalent aggressive anion besides Cl^- anions.

3.2. Influence of inorganic passivators

Generally, some inorganic salts are utilized as inhibitors to control the induced localized pitting corrosion current of C-steel in oilfield-produced water. The effect of the inorganic passivators is characterized by their impact on each induction time and the produced corrosion current. Fig. 6 depicts the variance in the pitting corrosion current density (µA cm^{-2}) with the immersion time of C-steel in oilfield produced water (50% FW) containing different additions

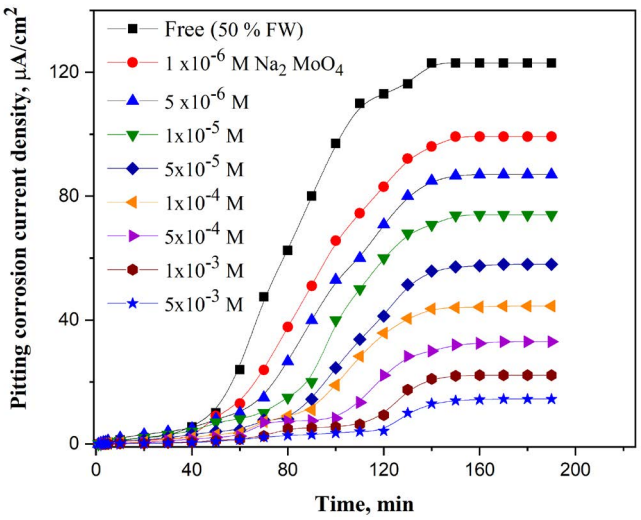

Fig. 6. Current-time curves for *C*-steel in % 50 FW containing different additions of $(NH_4)2MoO_4$, at 25°C.

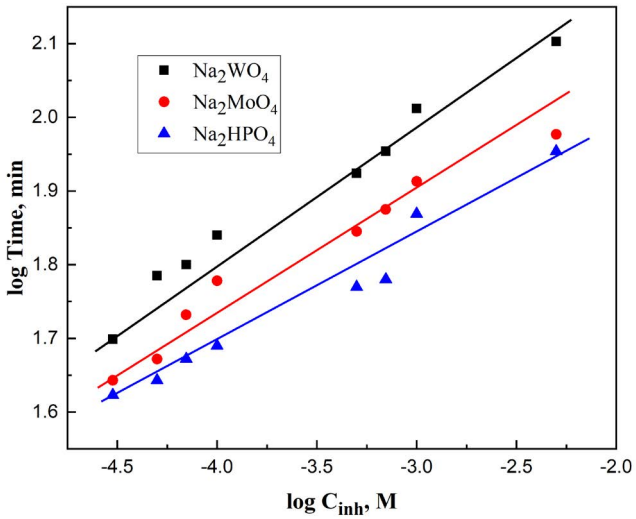

Fig. 7. Variation of the logarithm of the induction period on the logC_{inh} for C-steel immersed in 50% diluted oilfield formation water, at 25°C.

of Na_2MoO_4, at 25°C. Comparable data were gained when Na_2HPO_4 and Na_2WO_4 are added (curves are not shown).

Screening of the data of Fig. 6, signalizes that the existence of inorganic passivators gives rise to elongating the induction time accompanied with the initiation of the localized pitting corrosion and suppressing the current accompanied the pit propagation. Such behavior explains that the added inorganic passivators act as effective inhibitors towards the localized pitting corrosion of the C-steel immersed in the oilfield-produced water. More addition of the inorganic salts decreased the pitting corrosion currents to reach the minimum value confirming the passivation of the initiated formed pits.

The data of Fig. 7 depicts the variance of the logarithm of the incubation time, τ, required for the initiation of pitting against the logC_{inh}. Straight-lines are gained satisfying the relation [13]:

$$\log\tau = \zeta'' - \lambda'' \log C_{inh} \quad (4)$$

where ζ″ (minute unit) and λ″ (minutes/decade) are constants that depend on the solution composition and the metal under test.

Fig. 8 shows the variance of the logarithm of the limiting pitting corrosion current density, I_L with the logarithm of the amount of the inorganic passivators, C_{inh}. Straight-line relationships are gained obeying the relation:

$$\log I_L = \gamma - \delta \log C_{inh.} \quad (5)$$

where γ and δ are constants that depend on the kind of the used inhibitor and the metal under test, Table 3. The constant γ resembles the limiting current value, I_L, at C_{inh} equal to a molar concentration. The obtained value γ decreases in the sequence $Na_2WO_4 > Na_2MoO_4 > Na_2HPO_4$, which is congruent with the strength of the inhibition influence of the used salts against the initiation of pitting corrosion. It is clear that Na_2HPO_4 is the more effective inhibitor and Na_2WO_4 is the minimal.

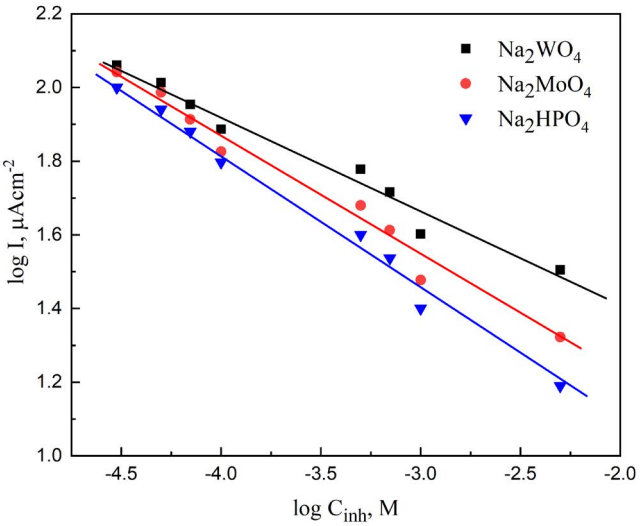

Fig. 8. Variation of the logarithm of the limiting-pitting corrosion current density, log*I*, with the logC_{inh} for C-steel in 50% diluted oilfield formation water, at 25°C.

Table 3
The values of the constants of Eq. (5) (γ, µA cm^{-2}, δ, µA cm^{-2}/decade and the correlation coefficient, R^2) and correlation coefficients, R^2, for inhibitors on C-steel surface in 50% FW, at 25°C

Type of salt	γ, µA cm^{-2}	δ, µA cm^{-2}/decade	R^2
Na_2HPO_4	0.35	–0.37	0.999
Na_2MoO_4	0.56	–0.33	0.988
Na_2WO_4	1.00	–0.25	0.977

The SEM micrograph of the C-steel samples after the period of the experiment when immersed in 50% diluted oilfield produce water containing 0.001 M Na_2HPO_4 is shown in Fig. 9, at 25°C. The micrograph indicated that the

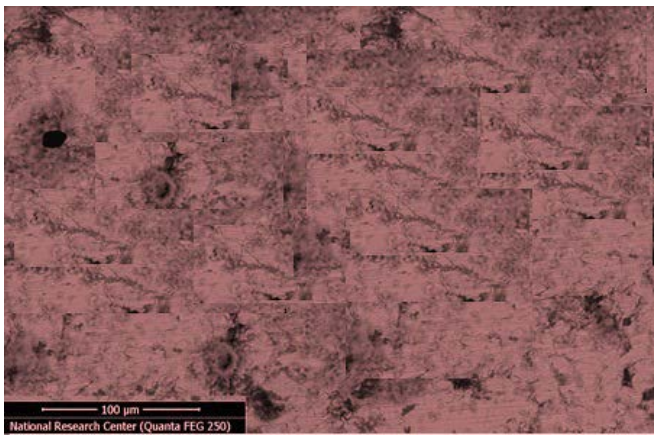

Fig. 9. SEM micrograph of C-steel surface after inundation for a period of 6 h in 50% diluted oilfield-produced water in the presence of 0.0001 M HPO_4^{2-} ions, at 25°C.

existence of Na_2HPO_4 reduces the number of pits in comparison with that obtained with the oilfield-produced water (free from inhibitor), Fig. 3.

The amplitude of inhibition towards the pitting corrosion of C-steel by the added salt could be estimated from the values of the surface coverage, θ, and the inhibition efficacy, η %. The values of θ and η % are deducted from the limiting current values in the inhibitor-free oilfield produced water, I_{L-free}, and in the existence of the inhibitor, I_{L-inh} according to Eqs. (6) and (7) [13,20].

$$\theta = \left(1 - \frac{I_{L-inh}}{I_{L-free}}\right) \quad (6)$$

$$\eta\,\% = (\theta)100 \quad (7)$$

The calculated values of θ and η % at various amounts of the added salts are listed in Table 4. Screening of such table reveals the following:

- Each of θ and η % values increases with increasing the concentration of the added salt.
- The inhibition efficiency η % increase in the sequence: Na_2WO_4 < Na_2MoO_4 < Na_2HPO_4, which is the consequence of the reduction in the values of the I_L values of Fig. 6 and similar ones.

3.3. Mechanism of inhibition

The presence of the inorganic salts decreases the localized pitting corrosion current density of C-steel in oilfield-produced water according to the order Na_2HPO_4 > Na_2MoO_4 > Na_2WO_4. This sequence is attributed to the rise in the ability of the corresponding anions to adsorb on the metal surface forming a protective layer that inhibits the localized pitting corrosion. HPO_4^{2-} is the more effective anion to tolerate localized pitting corrosion. The inhibition influence of the HPO_4^{2-} is of interest. Phosphate anions are rich with oxygen atoms and are theorized as oxygen-dependent inhibitors. HPO_4^{-2} ions can diffuse to the metal surface consuming most of the oxygen in their oxidation [42]. From another point of view, the charge on the steel surface beside the protonation state of phosphate ions inside the solution facilitates the adsorption of phosphate on the C-steel surface. The adsorption of such anions may be incorporated into the passive film to make it efficient for passivity against the destructive effect of aggressive ions naturally present in the oilfield-produced water [37]. Another way of inhibition effect of the HPO_4^{2-} anions could be attributed to the formation of a precipitate of $FeHPO_4$ on the C-steel surface that isolates the metal from the aggressive anions [38]. From another point of view, the existence of Na_2HPO_4 with higher concentrations behaves as an anodic inhibitor [28,38], that produces an insulating film on the C-steel surface formed from a mixture of γ-Fe_2O_3 and $FePO_3{\cdot}2H_2O$ [39,40].

Table 4
The values of the surface coverage, θ, and inhibition efficiency, η %, of different inhibitors on the corrosion of C-steel surface in 50% FW, at 25°C

Concentration, M	Na_2HPO_4		Na_2MoO_4		Na_2WO_4	
	θ	η %	θ	η %	θ	η %
3×10^{-5} M	0.187	18.7	0.104	10.4	0.065	06.5
4×10^{-5} M	0.292	29.2	0.211	21.1	0.163	16.3
7×10^{-5} M	0.382	38.2	0.333	33.3	0.268	26.8
1×10^{-4} M	0.490	49.0	0455	45.5	0.374	37.4
5×10^{-4} M	0.675	67.5	0.611	61.1	0.512	51.2
7×10^{-4} M	0.720	72.0	0.666	66.6	0.577	57.7
1×10^{-3} M	0.793	79.3	0.752	75.2	0.675	67.5
5×10^{-3} M	0.874	87.4	0.892	89.2	0.740	74.0

The mechanism of corrosion inhibition of the C-steel by molybdate anions was discussed before [41,43]. It is reported that the inhibition influence could be attributed to the reduction of hexavalent molybdenum ions into trivalent ions with the formation of molybdenum dioxide (MoO_2) which is inserted into the passive layer formed on the surface of the C-steel electrode [44]. In addition, the anodic and cathodic reaction that occurs in neutral aerated or basic solution (pH ≥ 7) can be represented by the following equations:

$$Fe \rightarrow Fe^{2+} + 2e^- \quad (I)$$

$$O_2 + H_2O + 4e^- \rightarrow 4OH^- \quad (II)$$

The dissolved O_2 can react with surface Fe atoms according to the equation:

$$2Fe + O_2 + 2H_2O \rightarrow 2FeOH^+ + 2OH^- \quad (III)$$

The produced $FeOH^+$ ions are unstable that can further be transformed into relatively stable oxide films Fe_2O_3/Fe_3O_4 [43]. The gradual accumulation of corrosion products on the C-steel surface forms a passive film that isolates the C-steel surface from the corrosive media and reduces the rate of pitting corrosion [45,46]. On the other hand, it cannot

be neglected that the MoO_4^{-2} ions are adsorbed electrostatically on the electrode surface anions forms a protective film on the steel surface [47].

The inhibiting action of tungstate is discussed frequently [11–14]. It was suggested that the primary adsorption of the WO_4^{2-} ions on the steel surface is accompanied by the formation of a passive iron tungstate, $FeWO_4$, that blocks the active sites on the metal surface [48] preventing pitting corrosion. However, the partial reduction of the WO_4^{2-} ions [49,50] to give lower valence tungsten oxide is believed to be incorporated into the passive film. Other authors [51,52] assumed that tungstate ions oxidize ferrous ions to a higher valence ferric state that facilitated more passivity of steel. However, Abd El Kader et al. [53] argued that the inhibition by tungstate necessitates the simultaneous presence of O_2 in solution and the formation of an ordered arrangement of the two species on the steel surface

3.4. Adsorption isotherm

Generally, the corrosion inhibition of most inhibitor molecules is directly associated with an adsorption process [54]. Such an adsorption process could follow various models of adsorption isotherms, like Langmuir, Freundlich, Temkin, and Frumkin [55]. The surface coverage, θ can be deduced from the limiting current values, I_L, without and with the additions of inhibitors, as shown from Eq. (6) [18].

The obtained values of θ for all used salts confirmed the Langmuir model, Fig. 10. Such a model can follow the relation [56]:

$$\frac{\theta}{1-\theta} = K_{ads}\, C_{inh} \tag{8}$$

$$\frac{C}{\theta} = \frac{1}{K_{ads}} + C_{inh} \tag{9}$$

where K_{ads} represents the adsorption–desorption equilibrium constant, and C_{inh} is the equilibrium concentration of the added salts. Fig. 10 depicts straight lines relations between C_{inh} θ^{-1} vs. C_{inh} for all the utilized salts with slopes very near to one, confirming correlation coefficients very near to one, Table 5. The adsorption–desorption equilibrium constants, K_{ads} are deduced from the values of the intercept of these straight lines. The K_{ads} values may be considered as a measure of the power of the adsorption operation between the utilized inorganic anions and the C-steel surface [57]. The K_{ads} are found to be 6,849; 5,444 and 3,891 mol^{-1} for Na_2HPO_4, Na_2MoO_4, and Na_2WO_4, successively. Such a conclusion confirms that Na_2HPO_4 is more effective than Na_2MoO_4 followed by Na_2WO_4. The standard free energy of adsorption, $\Delta G°_{ads}$ can be deduced from the K_{ads} values of according to the relation [58]

$$K_{ads} = \frac{1}{55.5}\exp\left(\frac{-\Delta G_{ads}}{RT}\right) \tag{10}$$

where 55.5 represents the molar concentration of water, R is the universal gas constant and T is the temperature in the kelvin scale. The calculated values of $\Delta G°_{ads}$ are −31.83, −31.26, and −30.44 kJ mol^{-1} for Na_2HPO_4, Na_2MoO_4, and Na_2WO_4, successively. This is proportionate with the higher inhibition efficacy of Na_2HPO_4 followed by Na_2MoO_4 and Na_2WO_4. The negative signs of $\Delta G°_{ads}$ confirm the spontaneity of the adsorption process on the C-steel surface with the constancy of the adsorbed film on the C-steel surface. The obtained values of $\Delta G°_{ads}$ are consistent with a chemisorption process due to chemical bond formation between the used anions and the metal surface [59–61].

Table 5
The adsorption–desorption equilibrium constant, K_{ads}, the free energy of adsorption, ΔG_{ads}, and correlation coefficient, R^2, of the inorganic salts on C-steel surface in 50% diluted oilfield formation water, at 25°C

Type of salt	K_{ads}, mol	$-\Delta G_{ads}$, kJ mol^{-1}	R^2
Na_2HPO_4	6,849	31.83	0.998
Na_2MoO_4	5,444	31.26	0.999
Na_2WO_4	3,891	30.44	0.997

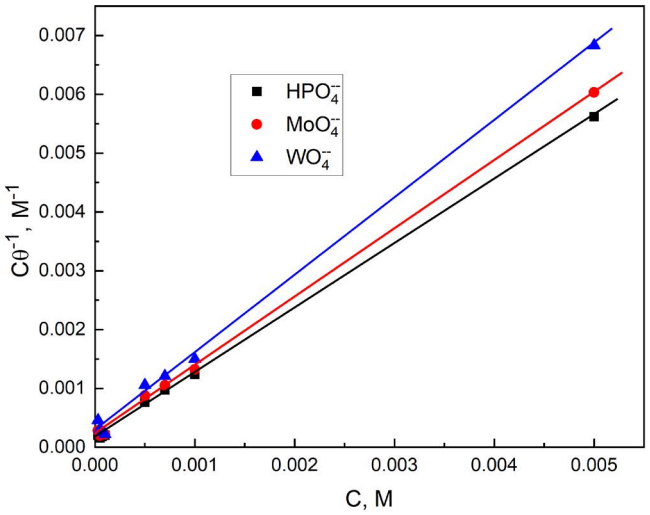

Fig. 10. Langmuir adsorption isotherm, C_{inh}/θ vs. C_{inh} for all used salts.

3.5. Effect of temperature

The influence of temperature on the pitting corrosion current of oilfield-produced water was investigated without and with the various additions of inorganic salts. The curves of Fig. 11 represent the *I–t* curves for C-steel in 50% diluted oilfield-produced water at various temperatures. On the other hand, Fig. 12 depicts the *I–t* curves for C-steel in 50% diluted oilfield-produced water containing 1 × 10^{-4} M Na_2WO_4 at various temperatures. Similar curves are gained with other used salts Na_2MoO_4, and Na_2HPO_4 (curves not shown). The induction period in all examined solutions (without and with inhibitor) preceding the pitting corrosion process decreases with temperature followed by an increase in the pitting corrosion current till reaching a constant value, I_L, due to propagation of

pitting corrosion [34]. Such behavior could be attributed to the increase in the rate of corrosion of C-steel with temperature due to the rise in the rate of penetration of the corrosive species (Cl^- and S ions) to the passive oxide film with temperature [62]. The Limiting pitting corrosion current density, I_L, of C-steel in oilfield-produced water devoid of and containing 1×10^{-4} M of different inorganic salts is plotted against the temperature in Kelvin values, Fig. 13. The data of this figure confirms that the I_L is increased with the temperature in the case of aggressive and inhibitive solutions.

The data of the curves of Figs. 11–13 reveals that:

- The rise in the temperature reduces the induction period, τ, and increases the limiting corrosion current, I_L.

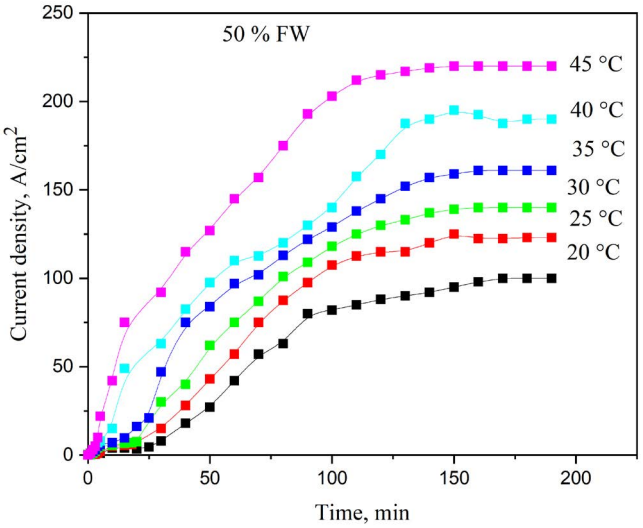

Fig. 11. *I–t* curves for C-steel in 50% diluted oilfield-produced water at various temperatures.

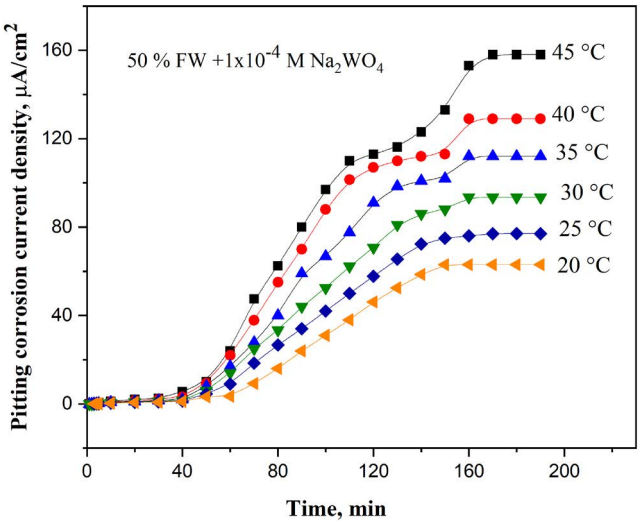

Fig. 12. *I–t* curves for C-steel in 50% diluted oilfield-produced water mixed with 0.0001 M Na_2WO_4 at various temperatures.

- In the aggressive and inhibitive solutions, the increase in the temperature rise the pitting corrosion current density due to the enhancement of the oxidation process ($Fe \rightarrow Fe^{+2} + 2e^-$).
- Various additives of Na_2HPO_4, Na_2MoO_4, and Na_2WO_4 reduce the pitting corrosion current and I_L values although the rise in the pitting corrosion current with temperature.
- The inorganic salts reduce the I_L values following the sequence: $Na_2HPO_4 > Na_2MoO_4 > Na_2WO_4$

Broadly, increasing the temperature for pitting corrosion enhances the initiation of pitting corrosion by reducing the induction period, τ, required pit formation, and enhancing the pit propagation by increasing the limiting pitting corrosion current density, I_L. The Arrhenius equation can be used to deduce the activation energy, E_a. Such an equation can be represented by the following relation [63]:

$$k = A \exp\left(-\frac{E_a}{RT}\right) \tag{11}$$

or

$$\log I_L = \log A - \frac{E_a}{2.303\,RT} \tag{12}$$

where the rate of reaction can be represented by I_L values, E_a is the activation energy of the pitting corrosion process, A is the Arrhenius constant, R is the ideal gas constant and T is the absolute temperature.

Fig. 14 depicts the variation of the logarithm of I_L vs. $1/T$ for 50% FW without and with various inorganic inhibitors (1×10^{-4} M). Straight-line relations are obtained confirming the Arrhenius equation. The slope of each line can be used to deduce the activation energy, E_a, required for pitting corrosion for all investigated electrolytes, Table 6 and correlation

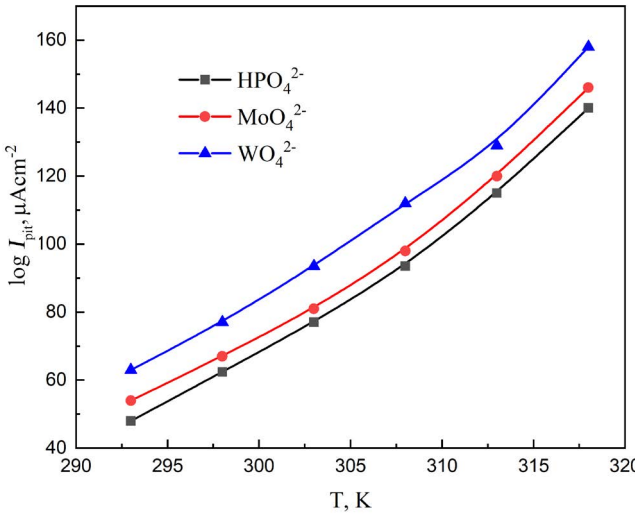

Fig. 13. Variation of the logarithm of the limiting pitting corrosion current density, logIpit with T, for C-steel in oilfield-produced water containing 0.0001 M of the used salts.

Table 6
Thermodynamic corrosion parameters, activation energy, E_a^* enthalpy of activation, ΔH^*, the entropy of activation, ΔS^*, and correlation coefficient, R^2, of C-steel in 50% FW without and with 0.0001 M of the used salts, at 25°C

Type of solution	E_a^*, kJ mol^{-1}	ΔH^*, kJ mol^{-1}	$-\Delta S^*$, J mol^{-1}	R^2
50% FW	23.51	21.40	169	0.992
50% FW + Na_2WO_4	27.98	25.40	165	0.997
50% FW + Na_2MoO_4	30.55	28.00	162	0.999
50% FW + Na_2HPO_4	32.50	30.16	159	0.998

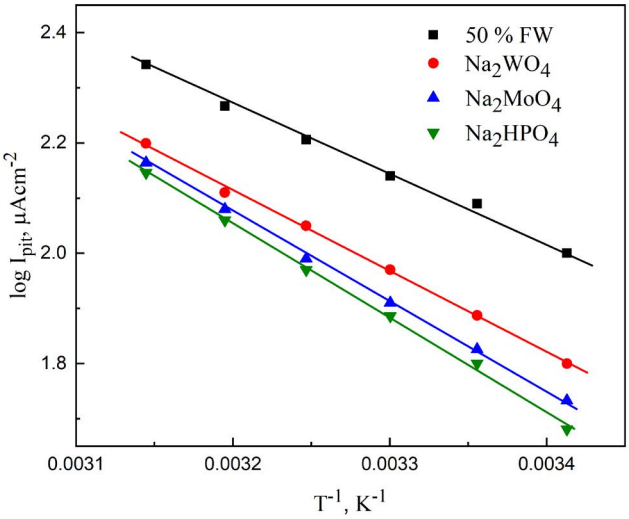

Fig. 14. The Arrhenious plots, variation of the logarithm of I_{pit} vs. 1/T for 50% FW without and with 0.0001 M of the various inorganic salts.

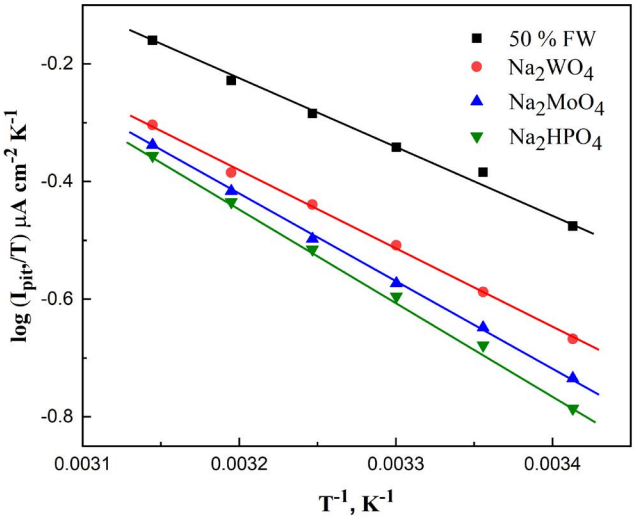

Fig. 15. Transition state plots, variation of the logarithm of I_{pit}/T vs. 1/T for 50% FW without and with 0.0001 M of the various inorganic salts.

coefficient, R^2, and correlation coefficient, R^2. The calculated value of E_a for the corrosion of C-steel in inhibitor-free oilfield-produced water is less than that obtained in presence of the added salts. Such behavior could be attributed to the increase in the energy barrier of the inhibitor being higher than those in the oilfield-produced water free of any additives. These anions tolerate the pitting corrosion of C-steel in oilfield-produced water due to competing with the aggressive anions (Cl^- and S) enhancing the oxide film repair and lowering the oxide film destruction [64]. The computed E_a accompanying the pitting corrosion increases in the order: 50% FW < Na_2MoO_4 < Na_2WO_4 < Na_2HPO_4. These additives were utilized as effective inhibitors towards the pitting corrosion of steel in calcium hydroxide [65] and zinc in sodium sulfate solutions [17].

Other thermodynamic parameters, entropy (ΔS_a) and enthalpy (ΔH_a) can be deducted when using transition state equation [66,67]:

$$\log\frac{I_L}{T} = \log\frac{R}{N_h} + \frac{\Delta S^*}{2.303R} - \frac{\Delta H^*}{2.303RT} \quad (13)$$

where N is the Avogadro's number, R is the universal gas constant, and h is the Plank's constant. Plotting of logI_L T^{-1} vs. 1/T for 50% FW without and with the various inorganic inhibitors (1 × 10^{-4} M) gives straight-line relations, Fig. 15. The slope of the gained plots represents the value of $\Delta H^*/2.303R$ while the intercept is equal to $(\Delta S^*/2.303R) + \log R/N_h$. The values of ΔH^* and ΔS^* are computed and tabulated in, Table 6. The activation adsorption entropy ΔS^* is determined to be –144.75 J mol K^{-1} for the inhibitor-free 50% FW and are –177.2, –168.6, and –164 J mol K^{-1} for the inhibitive solution Na_2MoO_4, Na_2WO_4, Na_2HPO_4, respectively. The negative values of ΔS_a in the case of inhibitor-free oilfield-produced water and with the inorganic salts confirm that that the activated complex in the rate-determining step represents an association rather than dissociation. Such attitude is due to the reduction in the disordering that takes place [67–69]. The positive values of ΔH^* confirm that the transition state (the activated complex) is an endothermic process.

4. Conclusions

The pitting corrosion current density for C-steel in the oilfield-produced water without and with the additions of Na_2MoO_4, Na_2WO_4, and Na_2HPO_4 was followed with the immersion time. The obtained data indicated that:

- The existence of an induction period preceding the pit formation. The increase in the corrosion currents depends

on the percent of dilution of the oilfield-produced water, the concentration of the inhibitive anions, as well as, the temperature of the solution.

- The limiting pitting corrosion current density, I_L decreases with the amount of the added inhibitive anions following the equation: $\log I_L = \zeta' + \lambda' \log C_{FW}$ %, where ζ' and λ' are constants.
- The induction period, τ, required for the initiation of pitting increases with increasing the amount of the added salts, C_{inh}.
- The inhibition efficiency is reduced in the order: $Na_2HPO_4 > Na_2MoO_4 > Na_2WO_4$.
- The activation energy accompanied by the pitting corrosion is increased in the order: $Na_2WO_4 < Na_2MoO_4 < Na_2HPO_4$

Disclosure statement

The authors declare no potential conflict of interest in preparing this article.

References

[1] S.M. Shaban, E.A. Badr, M.A. Shenashen, A.A. Farag, Fabrication and characterization of encapsulated Gemini cationic surfactant as anti-corrosion material for carbon steel protection in down-hole pipelines, Environ. Technol. Innovation, 23 (2021) 101603, doi: 10.1016/j.eti.2021.101603.

[2] S.M. Shaban, M.F. Elbhrawy, A.S. Fouda, S.M. Rashwan, H.E. Ibrahim, A.M. Elsharif, Corrosion inhibition and surface examination of carbon steel 1018 via N-(2-(2-hydroxyethoxy) ethyl)-N,N-dimethyloctan-1-aminium bromide in 1.0 M HCl, J. Mol. Struct., 1227 (2021) 129713, doi: 10.1016/j.molstruc.2020.129713.

[3] E.A. Badr, H.H.H. Hefni, S H. Shafek, S.M. Shaban, Synthesis of anionic chitosan surfactant and application in silver nanoparticles preparation and corrosion inhibition of steel, Int. J. Biol. Macromol., 157 (2020) 187–201.

[4] A. Labena, A. Hamed, E.H.I. Ismael, S.M. Shaban, Novel gemini cationic surfactants: thermodynamic, antimicrobial susceptibility, and corrosion inhibition behavior against *Acidithiobacillus ferrooxidans*, J. Surfactants Deterg., 23 (2020) 991–1004.

[5] S. Abd El Wanees, A.B. Radwan, M.A. Alsharif, S.M. Abd El Haleem, Initiation and inhibition of pitting corrosion on reinforcing steel under natural corrosion conditions, Mater. Chem. Phys., 190 (2018) 79–95.

[6] S. Abd El Wanees, M.I. Alahmdi, M. Abd El Azzem, H.E. Ahmed, 4,6-Dimethyl-2-oxo-1,2-dihydro-pyridine-3-carboxylic acid as an inhibitor towards the corrosion of C-steel in acetic acid, Int. J. Electrochem. Sci., 11 (2016) 3448–3466.

[7] S. Abd El Wanees, A. Diab, O. Azazy, M.A. El Azim, Inhibition effect of N-(pyridine-2-yl-carbamothioyl) benzamide on the corrosion of C-steel in sulfuric acid solutions, J. Dispersion Sci. Technol., 35 (2016) 1571–1580.

[8] S.M. Shaban, I. Aied, A.H. Moustafa, H. Aljoboury, Some alginates polymeric cationic surfactants; surface study and their evaluation as biocide and corrosion inhibitors, J. Mol. Liq., 273 (2019) 164–176.

[9] W.P. Singh, J.O. Bockris, Toxicity Issues of Organic Corrosion Inhibitors: Applications of QSAR Model, NACE-96225, Paper Presented at the CORROSION 96, Denver, Colorado, March 1996.

[10] M.A. Deyab, R. Essehli, B. El Bali, Performance evaluation of phosphate $NaCo(H_2PO_3)_3{\cdot}H_2O$ as a corrosion inhibitor for aluminum in engine coolant solutions, RSC Adv., 5 (2015) 48868–48874.

[11] S. Abd El Wanees, S. Nooh, A. Farouk, S.M. Abd El Haleem, Corrosion inhibition of aluminum in sodium hydroxide solutions using some inorganic anions, J. Dispersion Sci. Technol., (2021), doi: 10.1080/01932691.2021.1914647.

[12] E.E. Abd El Aal, S. Abd El Wanees, A. Farouk, S.M. Abd El Haleem, Factors affecting the corrosion behavior of aluminium in acid solutions. II. Inorganic additives as corrosion inhibitors for Al in HCl solutions, Corros. Sci., 68 (2013) 14–25.

[13] S.M. Abd El Haleem, S. Abd El Wanees, E.E. Abd El Aal, A. Diab, Environmental factors affecting the corrosion behavior of reinforcing steel. IV. Variation in the pitting corrosion current in relation to the concentration of the aggressive and the inhibitive anions, Corros. Sci., 52 (2010) 1675–1580.

[14] M.A. Deyab, S.S. Abd El-Rehim, Inhibitory effect of tungstate, molybdate and nitrite ions on the carbon steel pitting corrosion in alkaline formation water containing Cl^- ion, Electrochim. Acta, 53 (2007) 1754–1760.

[15] S.A.M. Refaey, S.S. Abd El-Rehim, F. Taha, M.B. Saleh, R.A. Ahmed, Inhibition of chloride localized corrosion of mild steel by PO_4^{3-}, CrO_4^{2-}, MoO_4^{2-}, and NO_2^- anions, Appl. Surf. Sci., 158 (2000) 190–196.

[16] Z.H. Dong, X.P. Guo, J.X. Zheng, L.M. Xu, Investigation on inhibition of CrO_4^{2-} and MoO_4^{2-} ions on carbon steel pitting corrosion by electrochemical noise analysis, J. Appl. Electrochem., 32 (2002) 395–400.

[17] E.E. Abd El Aal, S. Abd El Wanees, Galvanostatic study of the breakdown of Zn passivity by sulfate anions, Corros. Sci., 51 (2009) 1780–1788.

[18] A.M. Shams El-Din, S.M. Abd El Haleem, J.M. Abd El Kader, Studies on the pitting corrosion of zinc in aqueous solutions II. Measurement of pitting corrosion currents operating under natural conditions, J. Electroanal. Chem., 65 (1975) 335–349.

[19] S. Abd El Wanees, A. Abd El Aal Mohamed, M. Abd El Azeem, A.N. Abd El Fatah, Pitting corrosion currents of tin in relation to the concentration of the inhibitive and corrosive anions under natural corrosion conditions, Int. J. Electrochem. Sci., 3 (2008) 1005–1015.

[20] S. Abd El Wanees, A.B. Radwan, M.A. Alsharif, S.M. Abd El Haleem, Initiation and inhibition of pitting corrosion on reinforcing steel under natural corrosion conditions, Mater. Chem. Phys., 190 (2017) 79–95.

[21] F.P. Glasser, K.K. Sagoe-Crentsil, Steel in concrete: Part II electron microscopy analysis, Mag. Concr. Res., 41 (1989) 213–220.

[22] A. Chen, F. Cao, X. Liao, W. Liu, L. Zheng, J. Zhang, C. Cao, Study of pitting corrosion on mild steel during wet-dry cycles by electrochemical noise analysis based on chaos theory, Corros. Sci., 66 (2013) 183–195.

[23] S. Abd El Wanees, A. Abd El Aal, E.E. Add El Aal, Effect of polyethylene glycol on pitting corrosion of cadmium in alkaline solution, Br. Corros. J., 28 (1993) 222–226.

[24] S.M. Abd El Haleem, A. Abd El Aal, Pitting corrosion currents on steel in relation to the concentration of the inhibitive and corrosive anions under natural corrosion conditions, Br. Corros. J., 14 (1979) 226–230.

[25] S.M. Abd El Haleem, A. El Kot, A.A. Abdel Fattah, W. Tayor, Variation of pitting corrosion on iron surface, Corros. Preven. Control, 33 (1986) 151–157.

[26] E.E. Abd El Aal, Measurements of pitting corrosion currents of zinc in near neutral media, Corros. Sci., 44 (2002) 2041–2053.

[27] E.E. Abd El Aal, S. Abd El Wanees A. Diab, S.M. Abd El Haleem, Environmental factors affecting the corrosion behavior of reinforcing steel III. Measurement of pitting corrosion currents of steel in $Ca(OH)_2$ solutions under natural, Corros. Sci., 51 (2009) 1611–1618.

[28] S.M. Abd El Haleem, S. Abd El Wanees, Chloride induced pitting corrosion of nickel in alkaline solutions and its inhibition by organic amines, Mater. Chem. Phys., 128 (2011) 418–426.

[29] P.C. Pistorius, G.T. Burstein, Metastable pitting corrosion of stainless steel and the transition to stability, Philos. Trans. R. Soc. London, Ser. A, 341 (1992) 531–559.

[30] S.T. Pride, J.R. Scully, J.L. Hudson, Metastable pitting of aluminum and criteria for the transition to stable pit growth, J. Electrochem. Soc., 141 (1994) 3029–3040.

[31] N.J. Laycock, R.C. Newman, Localised dissolution kinetics, salt films and pitting potentials, Corros. Sci., 39 (1997) 1771–1790.
[32] G.S. Frankel, L. Stockert, F. Hunkeler, H. Bohn, Perspective on metastable pitting of stainless steel, Corrosion, 43 (1987) 429–436.
[33] T. Li, J. Wu, G.S. Frankel, Localized corrosion: passive film breakdown vs. Pit growth stability, Part VI: Pit dissolution kinetics of different alloys and a model for pitting and repassivation potentials, Corros. Sci., 182 (2021) 109277, doi: 10.1016/j.corsci.2021.109277.
[34] D.E. Williams, C. Westcott, M. Fleischmann, Studies of the initiation of pitting corrosion on stainless steels, J. Electroanal. Chem., 180 (1984) 549–564.
[35] E. Williams, C. Westcott, M. Fleischmann, Stochastic models of pitting corrosion of stainless steels: I. Modeling of the initiation and growth of pits at constant potential, J. Electrochem. Soc., 132 (1985) 1796–1804.
[36] P.C. Pistorius, G.T. Burstein, Aspects of the effects of electrolyte composition on the occurrence of metastable pitting on stainless steel, Corros. Sci., 36 (1994) 525–538.
[37] G.S. Frankel, L. Stockert, F. Hunkeler, H. Bohni, Metastable pitting of stainless steel, Corrosion, 43 (1987) 429–436.
[38] J. Xu, L. Jiang, J. Wang, Influence of detection methods on chloride threshold value for the corrosion of steel reinforcement, Constr. Build. Mater., 23 (2009) 1902–1908.
[39] H. Rocha, The breakdown by chlorine ions of the passivation layers of austanic 18/8 Cr/Ni steels, Werkst. Korros., 11 (1960) 352–356.
[40] W. Schwenk, Theory of stainless steel pitting, Corrosion, 20 (1964) 129t–137t.
[41] K. Schwabe, G.Z. Ditez, Zur Passivität des Nickels, Z. Phys. Chem., 62 (1958) 751–759.
[42] J. Sinko, Challenges of chromate inhibitor pigments replacement, inorganic coatings, Prog. Org. Coat., 42 (2001) 267–282.
[43] H. Tristijanto, M. NoerIlman, P.T. Iswanto, Corrosion inhibition of welded of X-52 steel pipelines by sodium molybdate in 3.5% NaCl solution, Egypt. J. Pet., 29 (2020) 155–162.
[44] J. Augustynski, in: R.P. Frankenthal, J. Kruger, Eds., Passivity in Metals, Electrochemical Society, Princeton, NJ, 1987, p. 989.
[45] J. Yang, Y. Lu, Z. Guo, J. Gu, C. Gu, Corrosion behavior of a quenched and partitioned medium carbon steel in 3.5 wt.% NaCl solution, Corros. Sci., 130 (2018) 64–75.
[46] Y. Ma, Y. Li, F. Wang, The effect of β-FeOOH on the corrosion behavior of low carbon steel exposed in a tropic marine environment, Mater. Chem. Phys., 112 (2008) 844–852.
[47] F.B. Ravari, S. Mohammadi, A. Dadgarinezhad, Corrosion inhibition of mild steel in simulated cooling water by blends of molybdate, nitrite, and picrate as a new anodic inhibitor, Anti-Corros. Methods Mater., 59 (2012) 182–189.
[48] W.D. Robertson, Electrochem, molybdate, and tungstate as corrosion inhibitors and the mechanism of inhibition, J. Electrochem. Soc., 98 (1951) 91–100.
[49] E. Ose, T. Yu. Zimina, M.N. Fokin, Dissolution, and inhibition of iron in a neutral solution containing nonstoichiometric surface oxides, Zashch Met., 21 (1985) 909–913.
[50] G.D. Wilcox, D.R. Gabe, Passivation studies using group V1A anions. Part V: Cathodic treatment of zinc, Br. Corros. J., 22 (1987) 254–258.
[51] K.K. Chew, D.R. Gabe, Alternatives to chromate for inhibition in deaerated acid solutions, Corros. Preven. Control, 26 (1979) 5–7.
[52] B. Jabeera, S.M.A. Shibli, T.S. Anirudhan, Synergistic inhibitive effect of tartrate and tungstate in preventing steel corrosion in aqueous media, Appl. Surf. Sci., 252 (2006) 3520–3524.
[53] M. Abd El Kader, A.A. El Warraky, A.M. Abd El Aziz, Corrosion inhibition of mild steel by sodium tungstate in neutral solution. Part 1: Behaviour in distilled water, Br. Corros. J., 33 (1998) 139–144.
[54] S Abd El Wanees, EE Abd El Aal, N-Phenylcinnamimide and some of its derivatives as inhibitors for corrosion of lead in HCl solutions, Corros. Sci., 52 (2010) 338–344.
[55] O.I. Balytes, O.O. Krokhrnal'nyl, Pitting corrosion of 12Kh 18AG 18Sh steel in chloride solutions, Mater. Sci., 35 (1999) 389–394.
[56] S.M. Abd El-Haleem, S. Abd El-Wanees, Chloride induced pitting corrosion of nickel in alkaline solutions and its inhibition by organic amines, Mater. Chem. Phys., 128 (2011) 418–426.
[57] P.C. Pistorius, G T Burstein, Metastable pitting corrosion of stainless steel and the transition to stability, Philos. Trans. R. Soc. London, Ser. A, 341 (1992) 531–559.
[58] S. Abd El Wanees, A.A.H. Bukhari, N.S. Alatawi, S. Salem, S. Nooh, S.K. Mustafa, S.S. Elyan, Thermodynamic and adsorption studies on the corrosion inhibition of Zn by 2,2′-dithiobis(2,3-dihydro-1,3-benzothiazole) in HCl solutions, Egypt. J. Chem., 64 (2021) 547–559.
[59] S.T. Pride, J.R. Scully, J.L. Hudson, Metastable pitting of Al and criteria for the transition to stable pit growth, J. Electrochem. Soc., 141 (1994) 3028–3040.
[60] N.J. Laycock, R.C. Newman, Localised dissolution kinetics, salt films and pitting potentials, Corros. Sci., 39 (1997) 1771–1790.
[61] M.P. Ryan, D.E. Williams, R.J. Chater, B.M. Hutton, D.S. McPhail, Why stainless steel corrodes, Nature, 415 (2002) 770–774.
[62] Y. Zuo, S. Fu, The effect of potential on metastable pitting of amorphous Ni alloy, Corros. Sci., 39 (1997) 465–471.
[63] S. Abd El Wanees, S.H. Seda, Corrosion inhibition of zinc in aqueous acidic media using a novel synthesized Schiff base – an experimental and theoretical study, J. Dispersion Sci. Technol., 40 (2019) 1813–1826.
[64] S.M. Abd El-Haleem, S. Abd El-Wanees, A. Bahgat, Environmental factors affecting the corrosion behavior of reinforcing steel. V. Role of chloride and sulfate ions in the corrosion of reinforcing steel in saturated $Ca(OH)_2$ solutions, Corros. Sci., 75 (2013) 1–15.
[65] S.M. Abd El Haleem, S. Abd El Wanees, E.E. Abd El Aal, A. Diab, Environmental factors affecting the corrosion behavior of reinforcing steel II. Role of some anions in the initiation and inhibition of pitting corrosion of steel in $Ca(OH)_2$ solution, Corros. Sci., 52 (2010) 292–302.
[66] S. Abd El Wanees, N.M. El Basiony, A.M. Al-Sabagh, M.A. Alsharif, S. Abd El Haleem, Controlling of H_2 gas production during Zn dissolution in HCl solutions, J. Mol. Liq., 248 (2017) 943–952.
[67] S.M. Abd El Haleem, S. Abd El Wanees, A. Farouk, Hydrogen production on aluminum in alkaline media, Prot. Met. Phys. Chem. Surf., 57 (2021) 906–916.
[67] P.C. Pistorius, G.T. Burstein, Aspects of the effects of electrolyte composition on the occurrence of metastable pitting on stainless steel, Corros. Sci., 36 (1994) 525–538.
[68] C. Alonso, C. Andrade, M. Castellote, P. Castro, Chloride threshold values to depassivate reinforcing bars embedded in a standardized OPC mortar, Cem. Concr. Res., 30 (2000) 1047–1055.
[69] C. Alonso, M. Castellote, C. Andrade, P. Castro, Chloride threshold dependence of pitting potential of reinforcements, Electrochim. Acta, 47 (2002) 3469–3481.